Large-eddy simulations of combustion instability suppression by static turbulence control

By J. U. Schlüter

1. Motivation

1.1. *Combustion instabilities and coherent structures*

Current combustion research is focused on pollutant reduction and fuel efficiency. One strategy to achieve these goals is to use lean premixed flames instead of diffusion flames. However, one major drawback of lean premixed flames is their susceptibility to combustion instabilities (Putnam 1971; McManus *et al.* 1993). The control of combustion instabilities is crucial in order to progress towards highly-efficient, low-pollutant combustors.

There are several mechanisms suspected of leading to combustion instabilities, such as periodic inhomogeneities in the mixture fraction, pressure sensitivity of the flame speed and the formation of large-scale turbulent structures (Mugridge 1980; Büchner *et al.* 1993; Peters & Ludford 1983). While an attempt to suppress combustion instabilities in practical applications has to address all these sources, the current work focuses on coherent structures as the driving mechanism in creating noise.

In vortex-driven combustion instabilities (Poinsot *et al.* 1987) the roll-up of a coherent structure near the burner nozzle bundles an amount of unburned fresh gases inside and increases the flame surface dramatically (Fig. 1). As a result, the fresh gases burn rapidly at a very distinct moment. The sudden heat release creates an acoustic wave, which – given the proper time-lag – delivers an acoustic perturbation. The acoustic perturbation triggers the roll-up of the next coherent structure in the shear layer (Crow & Champagne 1971; Ho & Huang 1982; Ho & Huerre 1984) created near the edge of the burner nozzle.

The *Rayleigh criterion* can be used to determine whether this process is self-amplifying: if the sudden heat release is in phase with the acoustic wave creating the next inhomogeneity, then this cycle will be repeated with a certain frequency.

The consequences of unstable combustion are often troublesome due to the intense pressure-fluctuation levels which can occur, as well as increased heat transfer to the combustor surfaces (Lang *et al.* 1987; Büchner *et al.* 1993). These conditions can result in system performance degradation (for example: an increase in the lean blow-off limit or unsteadiness in thrust production in the case of a propulsion device), unacceptable vibration or noise levels, and, in the worst case, system failure due to structural damage (McManus *et al.* 1993). The numerical prediction of combustion instabilities is challenging and has been tried only on very simple geometries (Brookes *et al.* 1999; Veynante & Poinsot 1997; Angelberger *et al.* 2000).

1.2. *Active vs. static control*

So far, most control strategies for combustion instabilities are based on active control mechanisms (McManus *et al.* 1993). Active control is achieved by a sensor in the combustion chamber, which measures frequency and phase of a combustion oscillation. The

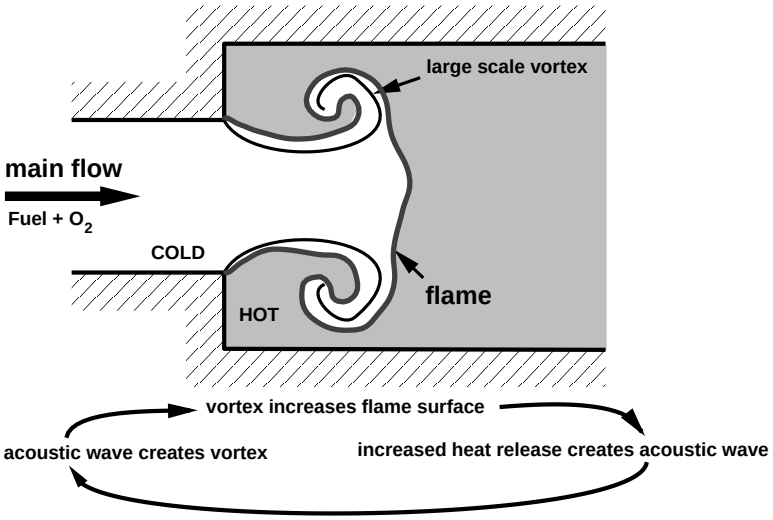

FIGURE 1. Sketch of coherent structures as the driving mechanism in combustion instabilities.

measured signal is then analyzed and a proper periodic response is determined. The response is either an acoustic perturbation or a modulation of the fuel supply (Paschereit *et al.* 1999). Active control is able to suppress combustion instabilities substantially and is already in use for numerous practical applications.

However, this apparatus for active control is rather expensive and maintenance-intensive. Furthermore, since a failure of the active control system can lead to a failure of the whole combustion system, this approach is not advisable for aircraft engines.

Static-control strategies are more robust and need a minimum of maintenance. With static control, a burner can be designed which is naturally less prone to combustion instabilities. However, to give design guidelines for static control, more information on this type of control has to be gathered.

1.3. *Static-control strategies*

Several strategies to control shear layers are known. The method that has received most attention is to use non-circular nozzle shapes like triangles (Schadow *et al.* 1988; Gutmark *et al.* 1989) and ellipses (Husain & Hussain 1983; Hussain & Husain 1987). However, the design of swirl combustors calls for axisymmetric nozzle shapes in order to generate swirl efficiently.

Other strategies involve hardware installations inside the shear layer. Honeycombs have had success in straightening the flow and destroying coherent structures efficiently (Nieberle 1986). The installation of these devices in practical burners is rather difficult, since they would have to be placed in the flame front. The excessive heat these devices would have to sustain makes the application of these installations unlikely.

One possibility of altering the nature of the shear layer fundamentally is to use a small slit near the edge at the backward-facing side of the step. Suction is a very efficient way to deflect the flow and to avoid large scale structures. However, in a premixed burner it would inevitably mean that fresh cold gases at a temperature close to the ignition point are part of the fluid sucked out of the combustion chamber. The further treatment of these gases is problematic.

The current study investigates static control in the form of a small circumferential slit

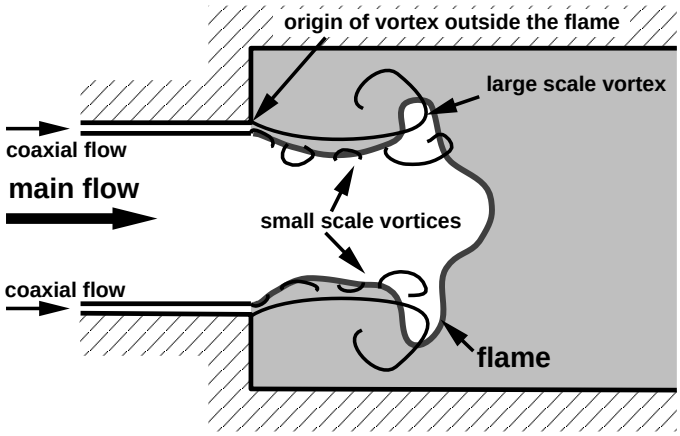

FIGURE 2. Static control by coaxial flow: The origin of large scale vortices is displaced outside the flame.

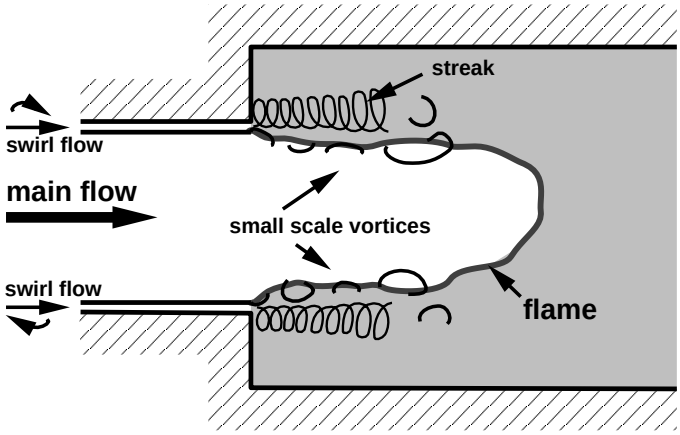

FIGURE 3. Static control by swirled coaxial flow: the generation of longitudinal streaks destroys large scale structures and enhances small scale mixing.

around the nozzle, *blowing* a coaxial flow into the combustion chamber. This coaxial flow carries less than 5% of the mass-flow rate of the main flow and can be used in two ways to control coherent structures:

(*a*) Displacement of the main shear layer (Fig. 2): the shear layer between the coaxial flow and the recirculation zone creates large-scale vortices, while the shear layer between main flow and coaxial flow creates less intense vortices, since the velocity difference is small. Although the intensity of coherent structures is unchanged, their influence decreases, since the origin of these vortices is outside of the flame front.

(*b*) Three-dimensionality of the shear layer (Fig. 3): by giving the shear layer a component in the third direction, e.g. by swirl, a second shear layer perpendicular to the main shear layer is created. As a result, a longitudinally-oriented vortex streak is created which disturbs vortex creation in the main shear layer (Fiedler 1998).

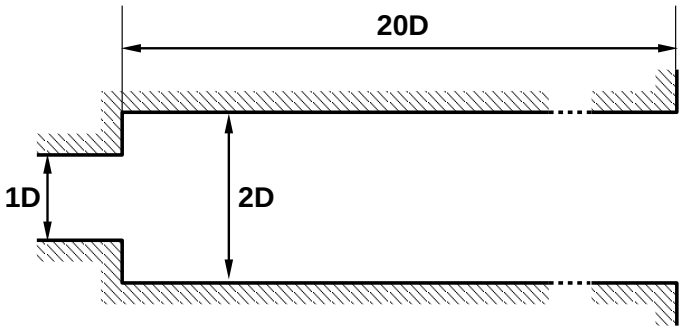

FIGURE 4. Geometry of the combustor

2. LES of static control

2.1. *Numerical tools for turbulence research*

Recent progress in numerical tools provides new elements in turbulence research. While flow solvers based on a Reynolds-averaged Navier-Stokes (RANS) formulation can predict the main flow features, Large Eddy Simulations (LES) are able to provide a detailed look at the origin, development, and decay of large scale turbulent structures. This allows a deeper insight into the dynamics which govern coherent structures, and ultimately can deliver answers on how to control the flow.

The advantage of numerical investigations over experiments is that a single parameter can be varied, leaving all other flow parameters unchanged. Experimental investigations usually encounter practical difficulties in achieving this goal.

Since the current work focuses on coherent structures as an origin of combustion instabilities, LES can be seen as the optimal tool to to find strategies to control large-scale structures in order to suppress combustion instabilities.

2.2. *Test case*

In order to obtain data about general ideas for static control, the current investigation examines a flow over an axisymmetric backward-facing step at a Reynolds-number $Re = 30,000$ (Fig. 4). This geometry corresponds to that used in an experimental investigation (Dellenback 1986; Dellenback *et al.* 1988) and extensive data for the cold flow are available.

While the experiments are carried out with both a non-swirling and a swirling flow, the LES computation focuses primarily on the non-swirled case, where vortex dynamics are better understood. The dynamics governing swirl flows are still controversial (Gupta *et al.* 1984; Keller 1995) and it is difficult to identify origin and control of a vortex structure in these flows.

2.3. *Strategy of the investigation*

It is difficult to examine naturally-excited combustion instabilities by numerical investigations. In the current investigation, therefore, the flow is forced in order to simulate periodic excitation by the combustion instability. A shear layer reacting to the periodic excitation amplifies the periodic disturbance. The quality of a static-control mechanism can be determined by the ability of the control mechanism to suppress the amplification of the excitation.

The external excitation of the flow makes it possible to determine the *potential* of a flame to create combustion instabilities. Whether a flame is finally unstable or not de-

pends on the ability of the heat release to create a periodic excitation that satisfies the Rayleigh criterion. The prediction of this feedback mechanism is tedious, since it involves computation of the acoustic wave propagation and knowledge of acoustic impedances at the boundaries of the computational domain. Here, for simplicity, acoustic effects have been explicitly excluded by using a flow solver based on a low-Mach number approximation. This makes it possible to have a detailed look at the one-way coupling between excitation and flame response. If using static control results in a reduction of the flame response to the excitation, a decrease of the ability of the flame to create an acoustic perturbation can be demonstrated, indicating a robustness against combustion instabilities.

In order to quantify the effect of a static-control device, the following procedure is employed.

First, the cold flow is examined. An LES computation of the test case is compared to the experimental data, to give an estimate of the accuracy of the applied approach.

Then, the excitation is carried out on the cold flow by a periodic modulation of the inlet profile. The shedding of coherent structures at the burner nozzle will lock into the forcing frequency, and a so-called triple decomposition can be applied to the flow variables (Hussain 1983). The instantaneous variable consists of three components; the time-independent component, the coherent (periodic) component and the incoherent turbulence:

$$f(x,t) = \bar{f}(x) + \tilde{f}(x,\phi) + f'_r(x,t) \tag{2.1}$$

where $\bar{f}(x)$ is the time-average of f, $\tilde{f}(x,\phi)$ the periodic component derived by phase-averaging, and $f'_r(x,t)$ the stochastic turbulent component.

Since $\tilde{f}(x,\phi)$ contains all periodic information about the excited flow, the kinetic energy of the periodic fluctuation:

$$\mathcal{E}(x,\phi) = \frac{1}{2}\left(\tilde{u}(x,\phi)^2 + \tilde{v}(x,\phi)^2 + \tilde{w}(x,\phi)^2\right) \tag{2.2}$$

can be computed, and its integral over all periods and the flow domain:

$$E_{per} = \int_0^{20D}\int_0^{2\pi} \mathcal{E}(x,\phi)\, d\phi\, dx \tag{2.3}$$

delivers the response of the flow system to a certain frequency. By several repetitions of the computation with different forcing frequencies, a transfer function can be determined.

In the third step, an LES computation of the cold flow with the static-control mechanism is performed. Again, several computations are made with different forcing frequencies and a transfer function is determined. The comparison of the two transfer functions delivers the effectiveness of the static-control mechanism on cold flow turbulence.

The fourth and final step involves the computation of a reacting flow field. Because of the high computational costs, only one example frequency is examined. Here the phase-averaged heat-release $\widetilde{\dot{Q}}$ delivers the flame response to the excitation. The comparison between uncontrolled and controlled flames and the comparison between reacting and non-reacting flows can deliver an answer on whether flame control via turbulence control is possible.

2.4. *LES flow solver and mesh*

For the current investigation, the LES flow solver developed at the Center for Turbulence Research (Pierce & Moin 1998) has been used. The code solves the filtered momentum

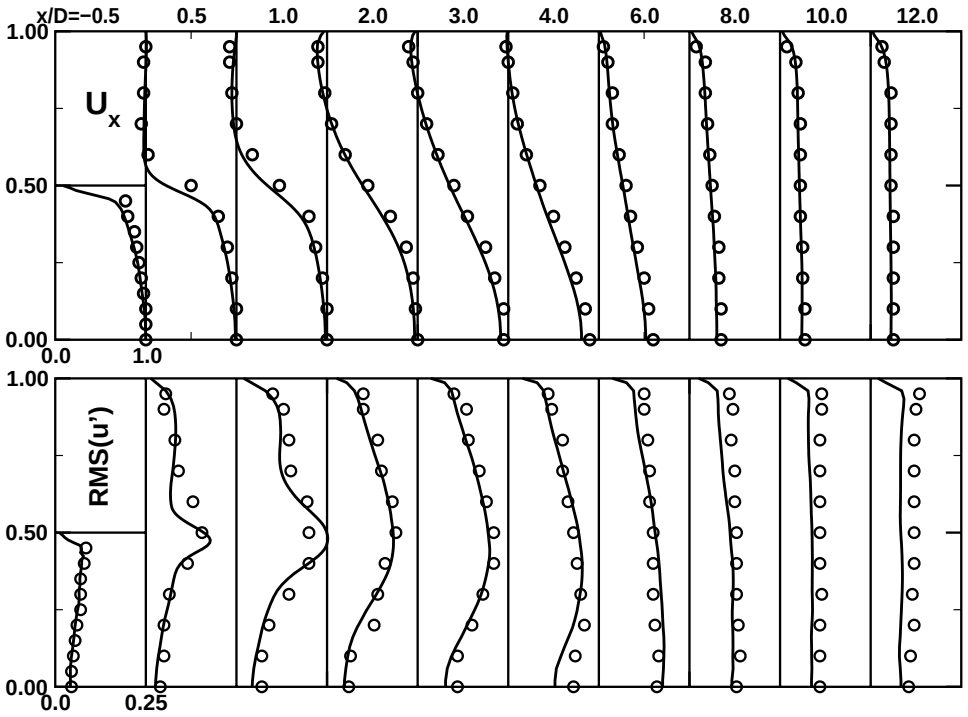

FIGURE 5. Above: mean axial velocity component $\bar{u}_x$, below: axial velocity fluctuations $\sqrt{\overline{u_x'^2}}$

equations with a low-Mach-number assumption on an axisymmetric structured mesh. As numerical method, a second-order finite-volume scheme on a staggered grid is used (Akselvoll & Moin 1996).

The subgrid stresses are approximated with an eddy-viscosity approach. The eddy viscosity is determined by a dynamic procedure (Germano *et al.* 1991; Moin *et al.* 1991).

In reacting cases, the G-equation approach is used to simulate a premixed flame. In the current case, a Bunsen burner flame has been assumed, using the same chemical characteristics as the LES computation of a similar flame (Duchamp & Pitsch 2000).

The geometry consists of an axisymmetric expansion (Fig. 4). The computational domain starts one diameter D upstream of the expansion and ends $10D$ downstream of the expansion in a convective outflow condition. The inflow velocity is generated by an independent LES computation of a periodic pipe flow which records the velocity components in the outflow plane and provides the data as inflow conditions.

The mesh consists of 384x64x64 cells, adding up to 1.6M cells. It is refined in regions of high shear, especially around the control slit. Mesh distribution of the flow with and without slit are exactly the same, with the exception of the control slit itself.

3. LES investigation on static control of the cold flow

3.1. *LES of a flow over an axisymmetric expansion*

Since experimental data are available for the cold flow of the chosen test case, the first step is to validate the LES flow solver against the experiments. Figure 5 shows a comparison of LES and experiments of the mean axial velocity and the axial-velocity fluctuations.

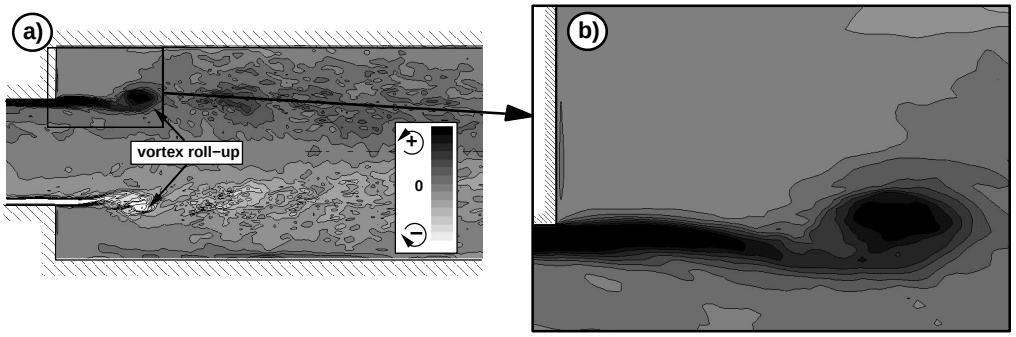

FIGURE 6. Natural, uncontrolled vortex roll-up. Non-reacting flow. Forcing frequency $St = 1.0$. Phase-averaged crosswise vorticity component $\tilde{\omega}_z$

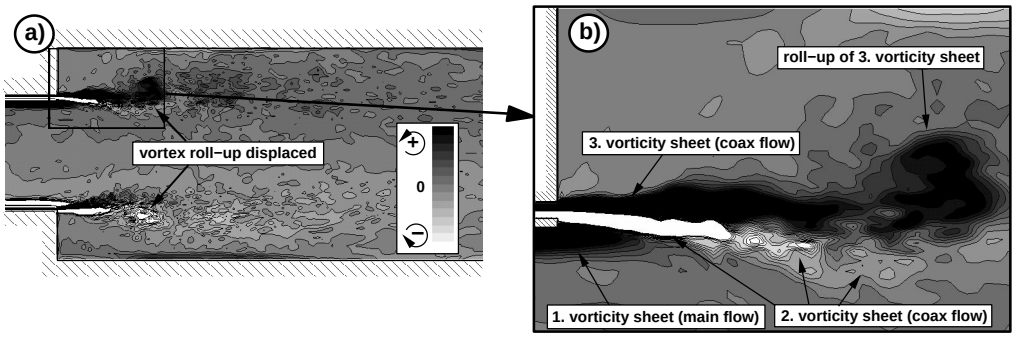

FIGURE 7. Static control by high-speed coaxial flow.($u_{coax} = 2u_{main}$). Non-reacting flow. Forcing frequency $St = 1.0$ Phase-averaged crosswise vorticity component $\tilde{\omega}_z$

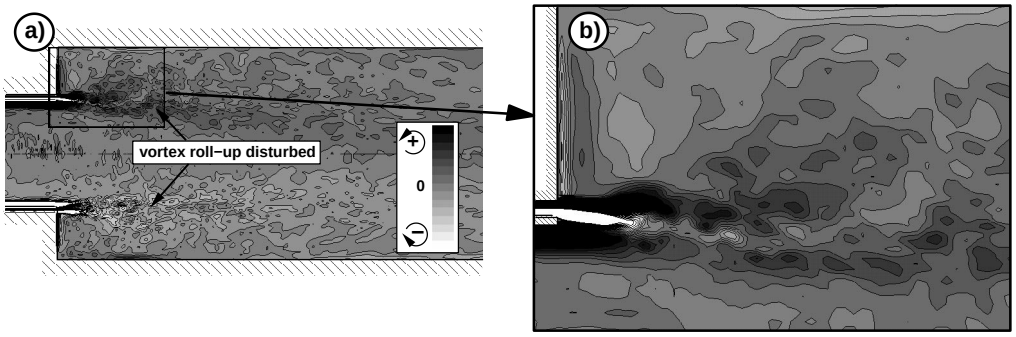

FIGURE 8. Static control by swirled coaxial flow ($u_{coax} = 1 \cdot u_{main}$, swirl number $S = 0.25$). Non-reacting flow. Forcing frequency $St = 1.0$ Phase-averaged crosswise vorticity component $\tilde{\omega}_z$

The mean axial-velocity component of the LES computation shows good agreement with the experiments, although the spreading rate of the shear layer behind the step is underestimated. The computed axial-velocity fluctuations also show good agreement with the experiment. However, the two profiles directly behind the step at $x/D = 0.5$ and $x/D = 1.0$ show some disagreements in shape. The highly-turbulent nature of the flow in this region complicates measurements and computations alike.

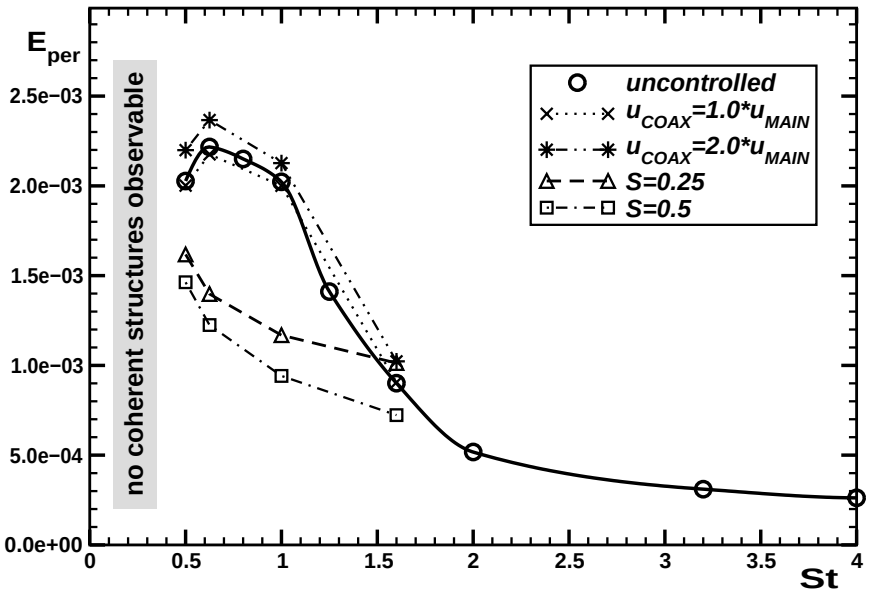

FIGURE 9. Kinetic energy E_{per} of the periodic perturbation (see eq. (2.3)) for different Strouhal-numbers $St = f \cdot D/U$

3.2. *Flow response to forcing*

Forcing the flow triggers the roll-up of coherent structures in the shear layer created by the main jet flow and the recirculation zone at the step. In order to determine the amplification of the forcing by the shear layer, the results of the LES computation are phase-averaged. The phase-averaging begins five periods after the flow forcing has been started, to allow for adjustment to the periodic excitation. The averaging is then carried out over 30 periods. A separate study showed that this number of periods is sufficient to obtain a statistically-converged phase average.

In order to visualize the vortex creation, Fig. 6a shows the the phase-averaged crosswise vorticity. The development of vortex rings with the forcing frequency can be seen. Dark spots denote counterclockwise-turning eddies and light spots clockwise-turning eddies. A close-up of the upper part of the step (Fig. 6b) shows a vorticity sheet with positive sign (dark) created by the boundary layer and the shear layer between the main flow and the recirculation zone near the step. This vorticity sheet rolls up and creates a vortex ring, which is to be manipulated in order to control a flame.

The effect of a coaxial high-speed stream on the creation of a vortex ring can be seen in Fig. 7a. The coaxial flow, here with a bulk velocity twice as high as the main flow, creates two additional vortex sheets with opposite signs. The close-up in Fig. 7b shows how the vorticity sheet with negative sign (white) shields the main flow and restrains the vorticity sheet of the main flow from rolling up into a vortex. Instead, the outermost vorticity sheet originating in the coaxial flow rolls up. Since this vortex consists mainly of fluid emanating from the coaxial flow it will have less influence on the flame front than in the uncontrolled case. However, the intensity of the vortex ring created by the coaxial flow is of approximately the same intensity as the vortex ring in the main flow in the uncontrolled case.

Figure 8a shows the employment of a swirled coaxial flow as a static-control mechanism.

Here, the axial bulk velocity of the coaxial flow is the same as the bulk velocity of the main flow, and the swirl number S:

$$S = \frac{2}{R_i + R_o} \frac{\int_{R_i}^{R_o} r^2 \bar{u}_x \bar{u}_\phi dr}{\int_{R_i}^{R_o} r \bar{u}_x^2 dr} \tag{3.1}$$

is approximately $S = 0.25$, where u_x is the axial velocity component, u_ϕ the azimuthal velocity component, R_i the inner radius of the coaxial slit, and R_o the outer radius of the coaxial slit. The effect of shielding the main flow by a vorticity sheet of opposite sign is still present (Fig. 8). Additionally, the creation of a shear layer in the azimuthal direction disturbs the vortex roll-up of the coaxial flow, and a decrease of coherence in the vortex can be determined.

In order to quantify the effect of the control mechanisms, the kinetic energy of the periodic flow perturbation was computed and integrated over the volume behind the step. Figure 9 shows the results for different Strouhal numbers ($St = fD/U$).

The natural, uncontrolled flow is denoted by circles. The maximum kinetic energy occurs near $St = 0.625$. Below that Strouhal number, the vortices created by the forcing are disturbed by the proximity of the outer wall. For sufficiently low Strouhal numbers, no coherent structures can be observed.

With increasing Strouhal number, the coherent structures shed at the step get smaller, and thus their contribution to the periodic fluctuation of the flow decreases. Above a Strouhal number of $St = 2.0$ the importance of these coherent structures is low. A comparison with the literature shows that combustion instabilities in gas turbine burners occur in the same frequency range as the amplification of periodic disturbances found here (Paschereit *et al.* 1998; Schildmacher *et al.* 2000).

The effect of the unswirled coaxial flow is not reflected in this presentation, since the vortex development is not prevented, but displaced. The kinetic energy of the coaxial flow with the same bulk velocity as the main-flow $u_{coax} = u_{main}$ is identical with the kinetic energy of the uncontrolled flow (crosses in Fig. 9). A high-speed coaxial flow ($u_{coax} = 2 \cdot u_{main}$) even amplifies the flow response (stars in Fig. 9), since the velocity difference in the outer shear layer between the coaxial flow and the recirculation zone is even higher than in the uncontrolled flow. The effectiveness of this control measure has to be shown in reacting computations.

However, using a swirled coaxial flow shows great potential even in the cold flow. Even the low swirl number $S = 0.25$ results in a considerable damping of the flow response (triangles in Fig. 9). An increase of the swirl number decreases the flow response even more (squares in Fig. 9). Here it can be seen that the swirled coaxial flow is able to damp the flow response by more than 50% over a broad frequency range.

4. LES Investigation on static control of the reacting flow

Since the computation of reacting flows is much more expensive, a full analysis like that for the cold flow cannot be given here, and so far, only the computations of one control mechanism have been carried out: the high-speed coaxial flow. In a reacting flow, the coaxial flow can carry either fresh air or hot products. The injection of fresh air near the ignition point of the flame would alter the chemical reaction of the flame in comparison to the uncontrolled flow. Since the current investigation concentrates on the attempt to control a flame mechanically and not chemically, the coaxial flow in the

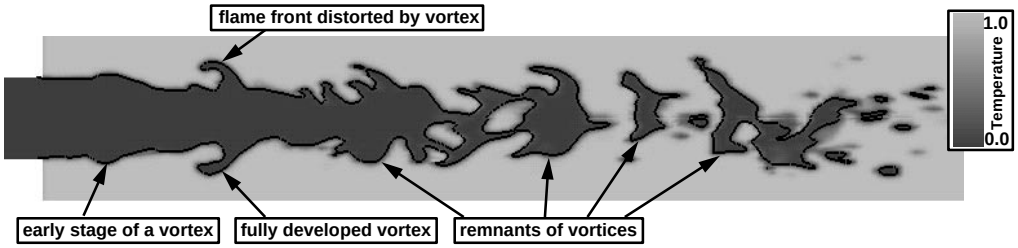

FIGURE 10. Uncontrolled flame. Instantaneous snapshot after 6 periods of forcing. Forcing frequency $St = 1.0$. Gray-scale: temperature T. Black line: G_0 (flame front).

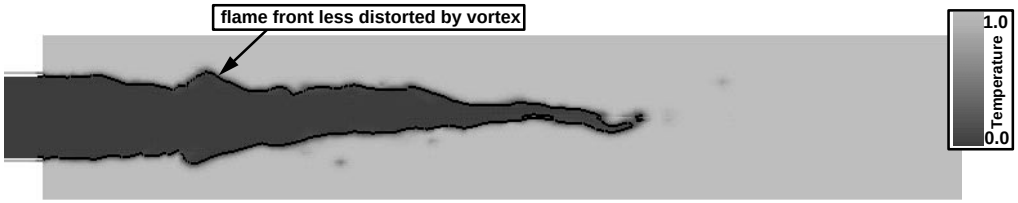

FIGURE 11. Static control by high-speed coaxial flow($u_{coax} = 2 \cdot u_{main}$). Instantaneous snapshot after 6 periods of forcing. Forcing frequency $St = 1.0$. Gray-scale: temperature T. Black line: G_0 (flame front).

computation carries hot products in order to provide the same chemical characteristics as the uncontrolled flame ignited by the recirculation zone at the dump.

The high computational costs prevent the computation of physical time-spans as long as in the cold flow. So far, the computed time-spans are shorter than the cold-flow counterparts, so a statistical analysis such as phase averaging contains more uncertainties.

Figure 10 shows an instantaneous snapshot of the temperature distribution of a periodically-excited flow. The influence of the vortices created by the forcing can be seen in different stages. In the beginning the vortices bulge the flame-front. Fully developed, the vortices create the typical mushroom-shaped distortion of the flame, and during their decay the vortices finally detach parts of the flame. These flame pockets float far downstream, where they are consumed.

Figure 11 shows the same flame with a high-speed coaxial flow. Large-scale vortices still distort the flame front, but have much less influence, since they are created outside the flame. Comparing Fig. 10 and Fig. 11, the most striking difference is that the flame with static control is more compact and seems much steadier than its uncontrolled counterpart, and no flame detachments take place. Since the small-scale mixing is enhanced by the coaxial flow, the flame length in this combustor is shorter than in the case without coaxial flow.

In order to give a quantitative measure on the efficiency of this control method the flow was averaged over nine periods. The turbulent kinetic energy of the periodic velocity fluctuations $\mathcal{E}$ was computed and integrated over all phase angles and over the volume of the combustion chamber. The employment of the coaxial flow resulted in a decrease of $\mathcal{E}$ by approximately 60% in comparison with the uncontrolled flow. This figure underlines the efficiency of the static-control method despite its simplicity.

Current investigations concentrate on the effect of control on the heat release and the influence of the swirled coaxial flow on the flame structure.

5. Conclusion

The static-control mechanism described here has proven to be an effective yet simple way to control turbulent coherent structures in a typical dump-combustor geometry. The installation of this static-control method is much easier than its active-control counterpart. The application of static control to reacting flows has shown great potential for suppressing periodic flame fluctuations.

Furthermore, LES has been a useful tool for understanding the mechanisms of vortex creation and suppression. Using a low-Mach-number code made it possible to explicitly exclude acoustic effects and pressure sensitivity of the flame, and to link the effects of the flame response directly to the forcing of the flow and the creation of large-scale vortices.

Future efforts will focus on the improvement and simplification of static control of reacting flames. Furthermore, the extension of these concepts to swirl combustors will be investigated.

REFERENCES

Akselvoll, K. & Moin, P. 1996 Large-eddy simulation of turbulent confined coannular jets. *J. Fluid Mech.*, **315**, 387-411.

Angelberger, C., Veynante, D. & Egolfopoulos, F. 2000 LES of chemical and acoustic effects on combustion instabilities. *Flow, Turbulence and Combustion* **65**, 205-222.

Brookes, S. J., Cant R. S. & Dowling, A. P. 1999 Modeling combustion instabilities using computational fluid dynamics. *ASME* 99-GT-112.

Büchner, H., Hirsch, C. & Leuckel, W. 1993 Experimental investigations on the dynamics of pulsated premixed axial flames. *Combust. Sci. and Tech.* **94**, 219-228.

Crow, S. C. & Champagne, F. H. 1971 Orderly structure in jet turbulence. *J. Fluid Mech.* **48**, 547-591.

Dellenback, P. A., Metzger, D. E. & Neitzel, G. P. 1988 Measurements in turbulent swirling flow through an abrupt axisymmetric expansion. *AIAA J.* **26**, 669-681.

Dellenback, P. A. 1986 Heat transfer and velocity measurements in turbulent swirling flows through an abrupt axisymmetric expansion. PhD thesis, Arizona State University.

Duchamp de Lageneste, L. & Pitsch, H. 2000 A level-set approach to large eddy simulation of premixed turbulent combustion. *Annual Research Briefs*, Center for Turbulence Research, NASA Ames/Stanford Univ., 105–116.

Fiedler, H. E. 1998 *Flow Control.* Control of Free Turbulent Shear Flows, (M. Gad-el-Hak, A. Pollard, & J. P. Bonnet, eds.), Springer, 335–429.

Germano, M., Piomelli, U., Moin, P. & Cabot, W., 1991 A dynamic subgrid-scale eddy viscosity model. *Phys. Fluids A* **3**, 1760-1765.

Gupta, A. K., Lilley, D. G. & Syred, N. 1984 *Swirl Flows.* Abacus Press.

Gutmark, E., Schadow, K. C., Parr, T. P, Hanson-Parr, D. M. & Wilson, K. J. 1989 Non-circular jets in combustion systems. *Expts. in Fluids* **7**, 248-258.

Ho, C. M. & Huang, L. S. 1982 Subharmonics and vortex merging in mixing layers. *J. Fluid Mech.* **119**, 443-473.

Ho, C. & Huerre, P. 1984 Perturbed free shear layers. *Ann. Rev. Fluid Mech.* **16**, 365-424.

Husain, H. S. & Hussain, A. K. M. F. 1983 Controlled excitation of elliptic jets. *Phys. Fluids* **26**, 2763-2765.

Hussain, A. K. M. F. 1983 Coherent structures – reality and myth. *Phys. Fluids* **26**, 2816-2849.

Hussain, A. K. M. F. & Husain, H. S. 1987 Passive and active control of jet turbulence. In *Turbulence Management and Relaminarisation*, (H. W. Liepmann and R. Narasimha, eds.), IUTAM Symposium Bangalore, India, 1987.

Keller, J. J. 1995 On the interpretation of vortex breakdown. *Phys. Fluids* **7**, 1695-1702.

Lang, W., Poinsot, T., Bourienne, F., Candel, S. & Esposito, E. 1987 Suppression of combustion instabilities by active control. *AIAA* Paper 87-1876.

McManus, K. R., Poinsot, T. & Candel, S. M. 1993 A review of active control of combustion instabilities. *Prog. Energy Combust. Sci.*, **19**, 1-29.

Moin, P., Squires, K., Cabot, W. & Lee, S. 1991 A dynamic subgrid-scale model for compressible turbulence and scalar transport. *Phys. Fluids A* **3**, 2746-2757.

Mugridge, B. D. 1980 Combustion driven oscillations. *J. Sound and Vibration* **70**, 437–452.

Nieberle, R., 1986 Entwicklung einer Methode der Mustererkennung zur Analyse kohärenter Strukturen und ihre Anwendung im turbulenten Freistrahl. *Fortschrittsberichte VDI*, Reihe 7: Strömungsmechanik (106), VDI Verlag.

Paschereit, C. O., Gutmark, E. & Weisenstein, W. 1998 Structure and control of thermoacoustic instabilities in a gas-turbine combustor. *Combust. Sci. and Tech.* **138**, 213-232.

Paschereit, C. O, Gutmark, E. & Weisenstein, W. 1999 Control of thermoacoustic instabilities in a premixed combustor by fuel modulation. *AIAA* Paper 99-0711.

Peters,N. & Ludford, G. S. S. 1983 The effect of pressure variations on premixed flames. *Combust. Sci. and Tech.* **34**, 331-344.

Pierce, C. D. & Moin, P. 1998 Large eddy simulation of a confined coaxial jet with swirl and heat release. *AIAA* Paper 98-2892.

Poinsot, T. J., Trouvé, A., Veynante, D., Candel, S. & Esposito, E., 1987 Vortex-driven acoustically coupled combustion instabilities. *J. Fluid Mech.*, **177**, 265-292.

Putnam, A. A. 1971 *Combustion Driven Oscillations in Industry.* American Elsevier.

Schadow, K. C., Gutmark, E., Parr, D. M. & Wilson, K. J. 1988 Selective control of flow coherence in triangular jets. *Expts. in Fluids* **6**, 129-135.

Schildmacher K.-U., Koch, R., Krebs, W., Hoffmann, S. & Wittig, S. 2000 Experimental investigations of the temporal air-fuel fluctuations and cold flow instabilities of a premixing gas turbine burner. *ASME* 2000-GT-84.

Veynante, D. & Poinsot, T. 1997 Large eddy simulation of combustion instabilities in turbulent premixed burners. *Annual Research Briefs*, Center for Turbulence Research, NASA Ames/Stanford Univ., 253-274.